

Magnetic properties and structure of $\text{LaNi}_{3/4}\text{Mn}_{1/4}\text{O}_3$

This article has been downloaded from IOPscience. Please scroll down to see the full text article.

2001 J. Phys.: Condens. Matter 13 L729

(<http://iopscience.iop.org/0953-8984/13/30/101>)

View [the table of contents for this issue](#), or go to the [journal homepage](#) for more

Download details:

IP Address: 171.66.16.226

The article was downloaded on 16/05/2010 at 13:59

Please note that [terms and conditions apply](#).

LETTER TO THE EDITOR

Magnetic properties and structure of $\text{LaNi}_{3/4}\text{Mn}_{1/4}\text{O}_3$ **J Blasco^{1,5}, J García¹, M C Sánchez¹, A Larrea², J Campo³ and G Subías⁴**¹ Instituto de Ciencia de Materiales de Aragón and Departamento de Física de la Materia Condensada, CSIC and Universidad de Zaragoza, 50009 Zaragoza, Spain² Instituto de Ciencia de Materiales de Aragón and Departamento de Ciencia de Materiales, CSIC and Universidad de Zaragoza, 50015 Zaragoza, Spain³ Institut Laue–Langevin, BP 156, 38042 Grenoble Cédex 9, France⁴ ESRF, BP 220, 38043 Grenoble, France

E-mail: jbc@posta.unizar.es

Received 11 April 2001, in final form 19 June 2001

Published 13 July 2001

Online at stacks.iop.org/JPhysCM/13/L729**Abstract**

We report here the structure and magnetic properties of $\text{LaNi}_{3/4}\text{Mn}_{1/4}\text{O}_3$. X-ray diffraction and transmission electron microscopy experiments demonstrate that this sample is a single perovskite phase and not a biphasic system as was thought in the past. The thermal evolution of the ac magnetic susceptibility shows two large magnetic anomalies at 45 and 262 K. Isothermal magnetization measurements indicate the presence of a very low ferromagnetic component below 262 K. The neutron diffraction experiments, instead, do not detect a magnetic contribution for this sample in the whole temperature range measured. The complex magnetic behaviour can be explained as a glassy ferromagnetic state, a phase with properties typical of both systems: ferromagnets and spin-glasses.

Ferromagnetism constitutes a rare property for mixed perovskite oxides. It has been found in magnetoresistive $\text{Ln}_{1-x}\text{A}_x\text{MnO}_3$ (Ln = lanthanide or trivalent cation; A = divalent cation) compounds [1] or in SrRuO_3 [2] but most of the other perovskite oxides are either antiferromagnetic or paramagnetic [3]. This scope has attracted a great interest over decades. Goodenough *et al* [4] reported the presence of ferromagnetism in $\text{LaMn}_{1-x}\text{M}_x\text{O}_3$ ($\text{M} = \text{Ni}, \text{Co}$) while the parent compounds are paramagnetic or antiferromagnetic. Blasse [5] suggested the ferromagnetism to be governed by the positive $\text{Ni}^{2+}(\text{Co}^{2+})\text{--O--Mn}^{4+}$ superexchange interaction. However, a controversy seems to exist about the existence of solid solution in $\text{LaNi}_{1-x}\text{Mn}_x\text{O}_3$ perovskites. These samples shows ferromagnetism ($0.1 \leq x \leq 0.9$) and the highest T_c corresponds to $x = 0.5$ (close to room temperature). The saturated magnetic moment instead, increases with increasing content of Mn. Vasanthacharya *et al* [6] claim the

⁵ Corresponding author: Dr Javier Blasco, Instituto de Ciencia de Materiales de Aragón and Departamento de Física de la Materia Condensada, CSIC and Universidad de Zaragoza, CL Pedro Cerbuna 12, 50009 Zaragoza, Spain.

presence of solid solution in the whole concentration range whereas another authors [7–9] argue that solid solution only exists for $x \geq 0.5$. Wold *et al* [7] reported that $\text{LaNi}_{1-x}\text{Mn}_x\text{O}_3$ samples with $x < 0.5$ are composed by two phases: an orthorhombic perovskite assigned to $\text{LaNi}_{1/2}\text{Mn}_{1/2}\text{O}_3$ and the rhombohedral perovskite LaNiO_3 . In the same way, Asai *et al* [8] suggested that x-ray patterns from $\text{LaNi}_{1-x}\text{Mn}_x\text{O}_3$ ($x < 0.5$) samples can be explained as the superposition of those of LaNiO_3 and $\text{LaNi}_{1/2}\text{Mn}_{1/2}\text{O}_3$. In addition, these authors noticed that the ferromagnetic moment decreases linearly with decreasing the Mn content while the Curie temperature almost remains constant. In spite of this strong evidence for phase segregation, Vasanthacharya *et al* only found single phases in their samples and spin-glass behaviour for low x values [6].

In order to give a definitive answer to this controversy, we have carried the present study on $\text{LaNi}_{3/4}\text{Mn}_{1/4}\text{O}_3$. Our aim is not only to determine the existence or otherwise of phase segregation but also a better understanding of the magnetic properties of this system.

Different $\text{LaNi}_{3/4}\text{Mn}_{1/4}\text{O}_3$ samples were prepared by means of a sol-gel route. Stoichiometric amounts of La_2O_3 , MnCO_3 and $2\text{NiCO}_3 \cdot 3\text{Ni}(\text{OH})_2 \cdot 4\text{H}_2\text{O}$ were dissolved in a nitric acid solution. Citric acid and ethylene-glycol were added in appropriate ratios and the solution was heated until the formation of a green gel. The gel was dried and the resulting brown powder was calcined overnight at 500°C in an oxygen current flow. Then, the powders were pressed into pellets and sintered, with intermediate grindings, at 900°C . Though different sintering times were used (48, 60, 90, 120 or 180 h), the resulting samples showed identical properties indicating the high reproducibility of the synthetic method. The oxygen stoichiometry was confirmed by thermogravimetric analysis in a reducing atmosphere ($\text{Ar}/\text{H}_2 = 95/5$). Figure 1 shows the x-ray pattern for $\text{LaNi}_{3/4}\text{Mn}_{1/4}\text{O}_3$ taken with a Rigaku D/max-B system and $\text{Cu K}\alpha$ radiation. The x-ray pattern is consistent with a single phase,

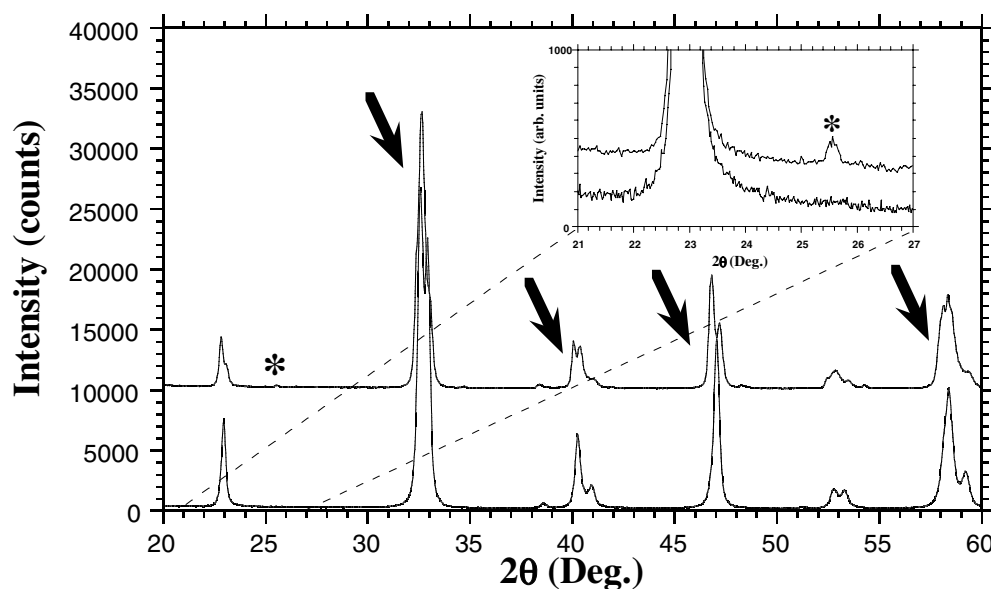


Figure 1. X-ray patterns at room temperature for $\text{LaNi}_{3/4}\text{Mn}_{1/4}\text{O}_3$ (bottom) and a mixture of $\text{LaNi}_{1/2}\text{Mn}_{1/2}\text{O}_3$ and LaNiO_3 (top). Arrows indicate the main differences. Inset: detail of the previous x-ray patterns showing the presence of an orthorhombic superstructure peak (asterisk) in the mixture.

a rhombohedral perovskite isostructural to LaNiO_3 , in agreement with Vasanthacharya *et al* [6]. We did not note any superstructure peak associated with an orthorhombic perovskite. The pattern of a mixture composed by LaNiO_3 and $\text{LaNi}_{1/2}\text{Mn}_{1/2}\text{O}_3$ (synthesized under the same conditions) is also displayed in figure 1. Both patterns are quite similar but several differences can be observed (for instance, the splitting indicated by arrows or the weak orthorhombic peak indicated by an asterisk). Therefore, the phase segregation into LaNiO_3 and $\text{LaNi}_{1/2}\text{Mn}_{1/2}\text{O}_3$ does not seem to be suitable to account for the $\text{LaNi}_{3/4}\text{Mn}_{1/4}\text{O}_3$ x-ray pattern. A pattern taken from 19° up to 120° with a step size of 0.02° and a counting rate of 6 s/step was analysed by the Rietveld method by using the Fullprof programme [10]. The refined unit cell parameters (hexagonal axes) were $a = 5.4826(2)$ and $c = 13.1985(3)$ Å. The refinement showed good profile, weighted and Bragg reliability factors (6.7, 8.6 and 3.2%, respectively). In order to verify the existence of this single phase, transmission electron microscopy (TEM) combined with x-ray energy dispersive spectroscopy (EDS) was used. Figure 2 shows a typical ~ 50 nm size crystal of $\text{LaNi}_{3/4}\text{Mn}_{1/4}\text{O}_3$. The inset shows the convergent beam electron diffraction pattern obtained when the crystal is oriented along the $[001]$ direction. This pattern can be indexed in a hexagonal unit cell in accordance with the x-ray diffraction study. No contrast produced by precipitates, intergrowths or any kind of phase segregation has been observed in any image. The cationic ratio of the compound was obtained from x-ray EDS microanalysis performed over ~ 7 nm size areas of the crystals. To determine this ratio the Cliff–Lorimer method [11] was applied to the La L, Mn K and Ni K characteristic fluorescence lines. The Cliff–Lorimer sensitivity factors (K_{MnLa} and K_{NiLa}) were experimentally measured using a $\text{LaNi}_{1/2}\text{Mn}_{1/2}\text{O}_3$ sample. In this conditions, several microanalysis were performed on the same crystal, allowing enough acquisition time to discard at 99.7% of confidence level that the micro-area analysed could be assigned to the $\text{LaNi}_{1/2}\text{Mn}_{1/2}\text{O}_3$, LaNiO_3 or LaMnO_3 phases. This study was extended over several crystals obtaining the same result. All the more than 30 spectra obtained are compatible with the $\text{LaNi}_{3/4}\text{Mn}_{1/4}\text{O}_3$ composition, leading to an overall result of $\text{LaNi}_{0.75\pm 0.02}\text{Mn}_{0.24\pm 0.02}\text{O}_3$. Therefore, $\text{LaNi}_{3/4}\text{Mn}_{1/4}\text{O}_3$ is single phase and solid solution exists for $\text{LaNi}_{1-x}\text{Mn}_x\text{O}_3$ samples with $x < 0.5$.

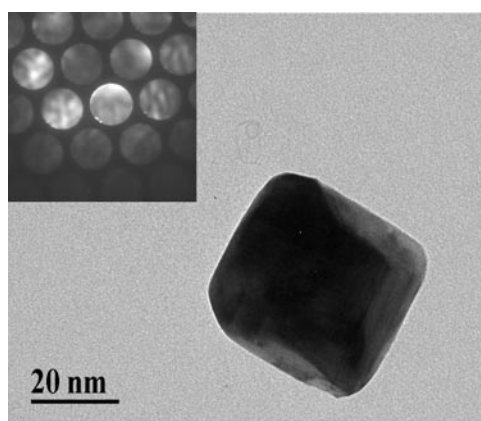


Figure 2. TEM photograph of a $\text{LaNi}_{3/4}\text{Mn}_{1/4}\text{O}_3$ crystal. Inset: convergent beam electron diffraction pattern obtained from the crystal oriented along the $[001]$ direction.

The magnetic properties of $\text{LaNi}_{3/4}\text{Mn}_{1/4}\text{O}_3$ have also been studied. Figure 3 displays the ac magnetic susceptibility for this sample. The in-phase, χ' , and out-phase, χ'' , (real and imaginary) components were measured in zero dc field with an alternating field of 4.5 Oe.

Different $\text{LaNi}_{3/4}\text{Mn}_{1/4}\text{O}_3$ samples qualitatively showed the same behaviour. A magnetic anomaly, typical of a ferromagnetic phase transition, is observed at 262 K (taken from the inflection point of the χ' curve). A second anomaly is observed at low temperatures: the χ' curve peaks around 45 K giving rise to a broad cusp. The χ'' curve also exhibits two peaks, one for each anomaly. The maximum of the low temperature peak is at 40 K. It is below the cusp temperature in the χ' curve as expected for a freezing process of magnetic moments. Surprisingly, the maximum for the high temperature peak is located at 250 K in the χ'' curve. It does not coincide with the inflection point of the χ' curve (as expected for a conventional para-ferromagnetic transition) but with the maximum of the magnetic anomaly in the χ' curve. In order to determine the magnetic ordering, neutron diffraction experiments were performed on this sample at the high flux reactor of the ILL (Grenoble). The D1B instrument was used with a pyrolytic graphite (002) focusing monochromator, giving a 2.52 Å wavelength. Patterns were recorded as temperature was slowly increased from 1.5 up to 300 K. The patterns were refined by using the Fullprof programme and the structural parameters were similar to the ones of the x-ray study. There is no remarkable difference between the patterns taken at room temperature and at 1.5 K. The intensities for all peaks remain unchanged, except for the thermal parameter effect. For instance, the thermal evolution of the intensity for the first ferromagnetic peak (110) is also displayed in figure 3(a). It is noteworthy that this peak shows a remarkable increase in its intensity below T_C for the ferromagnetic $\text{LaNi}_{1-x}\text{Mn}_x\text{O}_3$ ($x \geq 0.5$) compounds [12]. $\text{LaNi}_{3/4}\text{Mn}_{1/4}\text{O}_3$, instead, does not show any singular feature in the intensity of this peak down to 1.5 K. Moreover, no magnetic superstructure peaks were detected at low temperatures discarding an antiferromagnetic ordering. Therefore, any magnetic contribution, if exists, is very small. Either the correlation length is very short or the magnetic fraction is very small.

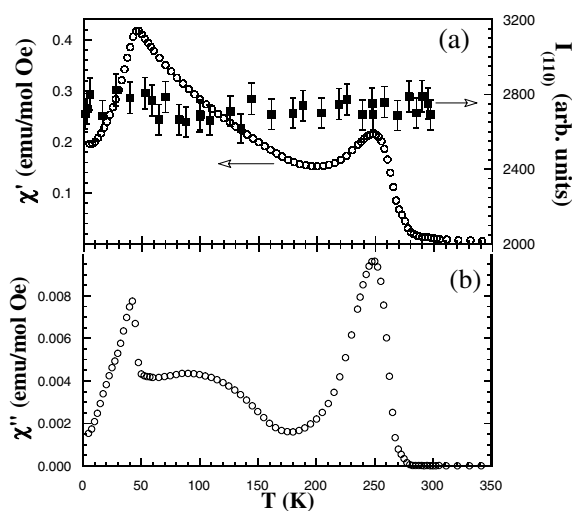


Figure 3. (a) Thermal dependence of the χ'_{ac} (in-phase component) and of the Bragg peak (110). (b) Thermal evolution of the out-of-phase component, χ''_{ac} . A frequency of 10 Hz was used.

In order to have a deeper understanding, we have performed different magnetization measurements. Figure 4(a) shows the isothermal magnetization curves at 5 K for different $\text{LaNi}_{3/4}\text{Mn}_{1/4}\text{O}_3$ samples. All of them show the same kind of curve suggesting an intrinsic behaviour that does not depend on the synthetic route (regrinding and refiring processes). In addition, our results compare quite well with the reported data [4, 6, 8] as expected for

an intrinsic behaviour. None of these samples show magnetic saturation at 5 K and at 5 T. The magnetic moment achieved at this field is around $0.4 \mu_B \text{ fu}^{-1}$, very far down from that expected for a fully polarized assembly of $\text{Ni}^{2+}/\text{Ni}^{3+}$ and Mn^{4+} ions. In addition, these samples have a large magnetic remanence. Figure 4(b) displays isothermal magnetization curves at different temperatures. A normal paramagnetic behaviour is observed above T_C (320 K) whereas none of the curves below T_C show magnetic saturation at 5 T. The isotherms below T_C are composed of two contributions: a spontaneous magnetization and a positive slope at high field. The positive slope decreases with increasing temperature as expected for a paramagnetic contribution superimposed on the weak ferromagnetic contribution. The spontaneous magnetization also increases as temperature decreases but a significant change is observed below 50 K. The isotherm at 5 K shows a large irreversibility and a large remanence. However, the remanence strongly decreases above 50 K (0.064, 0.007 and $\approx 0 \mu_B \text{ fu}^{-1}$ at 5, 50 and above 100 K, respectively) suggesting that the anomaly observed at 45 K in the χ' curve can be related to a freezing process of magnetic moments. In order to test this, magnetization measurements registered on warming in a dc field of 1 kOe after cooling in this field (FC) or after cooling without field (ZFC) were carried out. Figure 5 displays the results. The ZFC branch is similar to the χ' curve with a cusp around 45 K. The FC branch, instead, resembles a ferromagnetic compound with an almost constant magnetization at low temperatures. Accordingly, a large magnetic irreversibility is observed close to T_C . The inset of figure 5 shows the magnetization curve measured at 5 T. Though the freezing process is still observed at low temperatures, the ferromagnetic transition is completely smoothed.

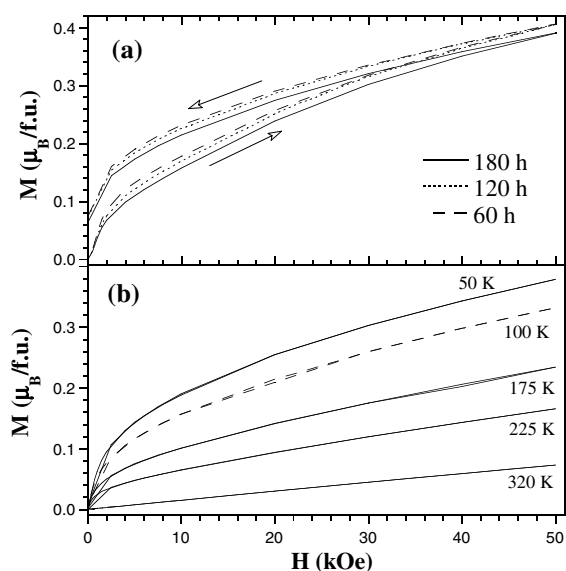


Figure 4. (a) Magnetization isotherms at 5 K for $\text{LaNi}_{3/4}\text{Mn}_{1/4}\text{O}_3$ samples with different sintering time (indicated in the plot). Arrows indicate the branches with increasing and decreasing magnetic field. (b) Magnetization isotherms at different temperatures (indicated in the figure) for the sample sintered 180 h at 900°C .

In order to gain insight into the magnetic properties of this system, ac susceptibility measurements at different frequencies (from 1 to 100 Hz) of the alternating field were carried out. Figure 6 shows the results. Dynamic behaviour was observed from the high-temperature anomaly down to the lowest temperature measured. However, both anomalies exhibit different

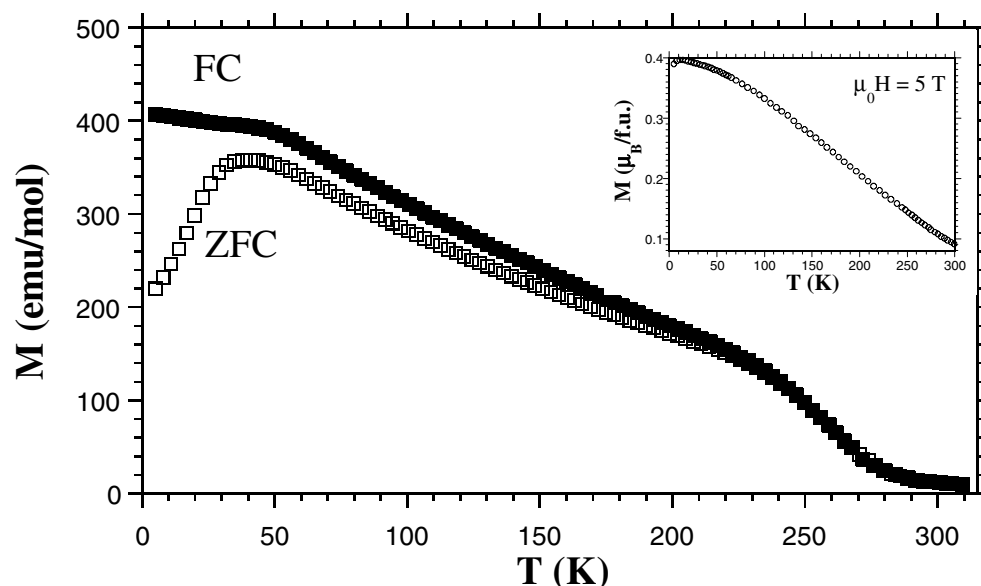


Figure 5. Thermal dependence of the magnetization of the $\text{LaNi}_{3/4}\text{Mn}_{1/4}\text{O}_3$ under an applied field of 1 kOe for increasing temperatures after cooling the sample in zero-field (ZFC) or under a field of 1 kOe (FC). Inset: magnetization against temperature under an applied field of 5 T (ZFC condition).

dynamic behaviour. The amplitude of the anomaly at 250 K depends on the frequency (it decreases as the frequency increases) but the position of the maximum is practically constant in this frequency range. The low temperature anomaly, instead, shows a shift of the maximum towards higher temperatures as the frequency increases. In order to characterize the relaxation phenomena, we have determined the term K , $K = \Delta T_f / [T_f \Delta(\log_{10} f)]$, T_f and f being the freezing temperature of spins (or clusters) and frequency of the alternating field, respectively. Δ refers to difference. We have estimated a value of $K = 2.5 \times 10^{-2}$, taking the cusp of the χ' curve. This value compares quite well with typical spin-glass systems [13] such as $(\text{LaGd})\text{Al}_2$ or $(\text{EuSr})\text{S}$. It is noteworthy that blocking processes of superparamagnetic particles usually have rather higher (at least, one order of magnitude) frequency dependence [13].

Let us summarize the magnetic properties of this compound. $\text{LaNi}_{3/4}\text{Mn}_{1/4}\text{O}_3$ shows a phase transition at 262 K suggesting a ferromagnetic ordering. However, long range ordering is not detected by neutron diffraction and the ac susceptibility curve is not characteristic of a conventional ferromagnet (maximum of the imaginary component and frequency dependence). Moreover, a freezing process of magnetic moments is clearly deduced from the magnetic behaviour at low temperatures. A reentrant phase transition from a ferromagnet to a spin-glass phase in a disordered ferromagnet could account for these features [14]. However, the thermal magnetic irreversibility in a reentrant system is usually observed at the freezing temperature [15] but $\text{LaNi}_{3/4}\text{Mn}_{1/4}\text{O}_3$ exhibits this irreversibility close to T_C . This sample presents randomness in the position of Mn and Ni atoms leading to bond disorder. In addition, competitive magnetic interactions are present due to the randomness and the intermediate valence state of transition metal ions [16]. Magnetic frustration due to competitive interactions (superexchange $\text{Ni}^{2+}\text{-O-Mn}^{4+}$ is ferromagnetic whereas $\text{Mn}^{4+}\text{-O-Mn}^{4+}$ is antiferromagnetic or $\text{Ni}^{3+}\text{-O-Ni}^{3+}$ is non-interacting in LaNiO_3 , for instance) together with randomness can lead

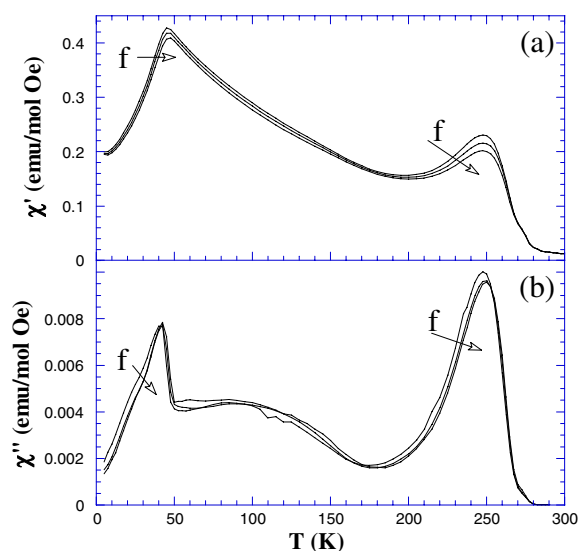


Figure 6. Ac magnetic susceptibility at different frequencies of the alternating field (1, 10 and 100 Hz) for a $\text{LaNi}_{3/4}\text{Mn}_{1/4}\text{O}_3$ sample sintered for 180 h at 900°C . Panel (a) shows the in-phase (real) component whereas panel (b) shows the out-of-phase (imaginary) component. Arrows indicate the frequency increase.

to a magnetic glassy state as occurs in related systems [17]. The ferromagnetism should be developed in small regions within a non-magnetic background. Random antiferromagnetic interactions cannot be discarded in such a background. The system then, exhibits both ferromagnetic and spin-glass properties. The ferromagnetic regions may show a large distribution of sizes but they are not large enough to give a significant contribution to the neutron patterns within the accuracy limits of our experimental set-up. However, the largest regions order at high temperature giving rise to the magnetic anomaly at 262 K. The complex magnetic behaviour at lower temperatures results from transitions and thermally freezing processes of ferromagnetic regions with different sizes.

Complex magnetic behaviour has also been reported for other related mixed oxides such as doped manganites [18–20] or cobaltates [21, 22]. They have been explained in terms of mictomagnetism or cluster-glass formation. In particular, the formation of ferromagnetic clusters seems to be favoured by the simultaneous presence of Mn and Ni atoms [18, 19]. However, additional effects, such as magnetocrystalline anisotropy, seems to play a role in these systems [22].

In summary, we have prepared different samples, whose composition is $\text{LaNi}_{3/4}\text{Mn}_{1/4}\text{O}_3$, exhibiting a complicated and intrinsic magnetic behaviour. TEM, EDS and x-ray diffraction studies have shown that these samples are single phases and not biphasic as reported in the past. Microcrystals with the accurate chemical composition demonstrates the existence of this phase and it strongly supports the presence of solid solution between Ni and Mn atoms in the whole $\text{LaNi}_{1-x}\text{Mn}_x\text{O}_3$ series. The magnetic properties of $\text{LaNi}_{3/4}\text{Mn}_{1/4}\text{O}_3$ can be considered as a mixture of ferromagnetic and spin-glass properties. The presence of both randomness and competitive interactions avoids the formation of a conventional ferromagnetic ground state and the resulting glassy ferromagnet shows the co-operative freezing of spins in a nontrivial pattern that is random in space without contribution to the magnetic Bragg peaks.

Fruitful discussions with F J Lázaro are acknowledged. This work has been supported by the Spanish CICYT under grant MAT99-0847. The Spanish CRG beam-time on D1B (ILL) is acknowledged for neutron experiments.

References

- [1] Rao C N R, Cheetham A K and Mahesh R 1996 *Chem. Mater.* **8** 2421.
- [2] Jonker G H 1956 *Physica* **22** 707
- [3] See for instance, Galasso F S 1969 *Structure, Properties and Preparation of Perovskite-Type Compounds (Solid State Physics Vol 5)* (Pergamon)
- [4] Goodenough J B, Wold A, Arnott R J and Menyuk N 1961 *Phys. Rev.* **124** 373
- [5] Blasse G 1965 *J. Phys. Chem. Solids* **26** 1969
- [6] Vasanthacharya N Y, Ganguly P, Goodenough J B and Rao C N R 1984 *J. Phys. C: Solid State Phys.* **17** 2745
- [7] Wold A and Arnott R J 1959 *J. Phys. Chem. Solids* **9** 176
- [8] Asai K, Sekizawa H and Iida S J 1979 *J. Phys. Soc. Japan* **47** 1054
- [9] Sonobe M and Kichizo A 1992 *J. Phys. Soc. Japan* **61** 4193
Fujiki H and Nomura S J 1967 *J. Phys. Soc. Japan* **23** 648
- [10] Rodríguez-Carvajal J L 1992 *Physica B* **55** 192
Rodríguez-Carvajal J L and Roisnel T <http://www-llb.cea.fr/fullweb/fullprof.98/fp98.htm>
- [11] Cliff G and Lorimer G W 1975 *J. Microsc.* **103** 203
- [12] Blasco J, García J, Sánchez M C, Subías G, Proietti M G and Campo J 1999 *ILL Experimental Report* CRG-381, <http://www.ill.fr>
- [13] Mydosh J A 1993 *Spin Glasses: an Experimental Introduction* (London: Taylor and Francis)
- [14] Hertz J A, Sherrington D and Nieuwenhuizen Th M 1999 *Phys. Rev. E* **60** R2460
- [15] Ryan D H 1992 *Recent Progress in Random Magnets* ed D H Ryan (Singapore: World Scientific Publishing) p 1
- [16] Sánchez M C, Subías G, Pérez-Cacho J, García J and Blasco J 2001 *J. Synchrotron Radiat.* **8** 901
- [17] Pérez J, García J, Blasco J and Stankiewicz J 1998 *Phys. Rev. Lett.* **80** 2401
- [18] Feng J-W and Hwang L-P 1999 *Appl. Phys. Lett.* **75** 1592
- [19] Wang Z-H, Shen B-G, Tang N, Cai J-W, Ji T-H, Zhao J-G, Zhan W-S, Che G-C, Dai S-Y and Ng D H L 1999 *J. Appl. Phys.* **85** 5399
- [20] Li X-G, Fan X J, Ji G, Wu W B, Wong K H, Choy C L and Ku H C 1999 *J. Appl. Phys.* **85** 1663
- [21] Señarís-Rodríguez M A and Goodenough J B 1995 *J. Solid. State Chem.* **118** 323
- [22] Anil Kumar P S, Joy P A and Date S K 1998 *J. Phys.: Condens. Matter* **10** L487